Frontiers in Bioscience Elite

Supplementary material

Developing SNEDDSs Comprising an Artemether-Lumefantrine Fixed-Dose Combination to Treat Malaria– Supplementary Material

Joe M. Viljoen [*], Lauren Cilliers and Lissinda H. du Plessis

[1]Faculty of Health Sciences, Centre of Excellence for Pharmaceutical Sciences (PharmacenTM), Building G16, North-West University, 11 Hoffman Street, Potchefstroom 2520, North-West Province, South Africa

*Correspondence: Joe.Viljoen@nwu.ac.za (Joe M. Viljoen)

[†]These authors contributed equally.

ORCID:
Joe Viljoen: 0000-0002-2489-1616
Lissinda du Plessis: 0000-0003-0954-2976

Frontiers in Bioscience Elite

Developing SNEDDSs Comprising an Artemether-Lumefantrine Fixed-Dose Combination to Treat Malaria – Supplementary Material

S1. Infrared (IR) Spectroscopy

An Alpha Sample Compartment RT-DLaTGS spectroscope (Bruker Alpha Sample Compartment RT-DLaTGS, USA) was employed to analyze the absorbance wavelengths of both active ingredients, artemether (ART) and lumefantrine (LUM). The resulting individual IR spectrums were compared to that of a reference standard by means of data overlays of the spectrums. Both ART and LUM were recognized and attested to be pure active ingredients without the presence of contamination as the peaks and peak intensities of both samples correlated to that of the individual reference standards. The absence of additional peaks at differing intensities excluded the presence of impurities as can be seen in Fig. S1 and S2.

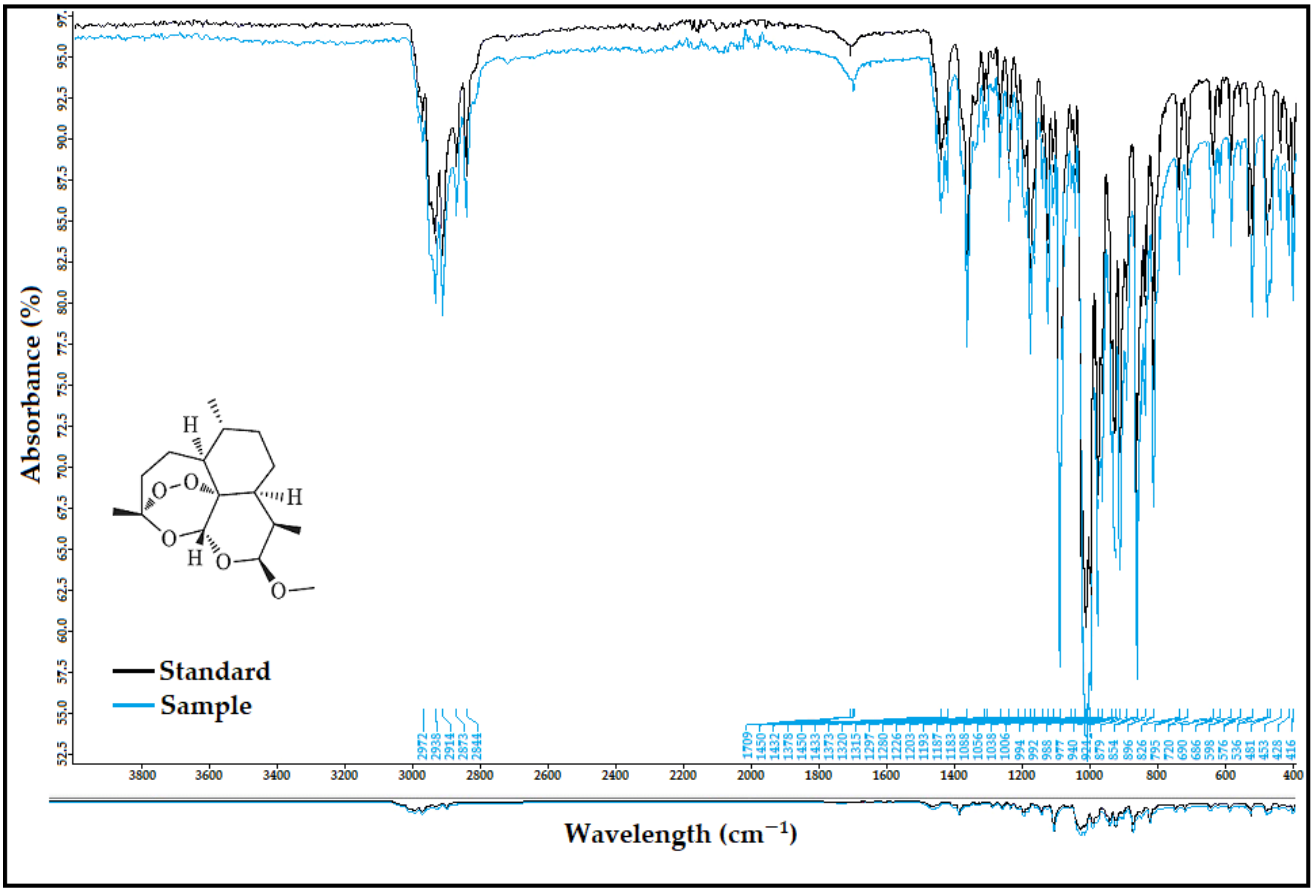

Fig. S1. IR spectra of both the artemether (ART) used in the study, as well as the ART reference standard.

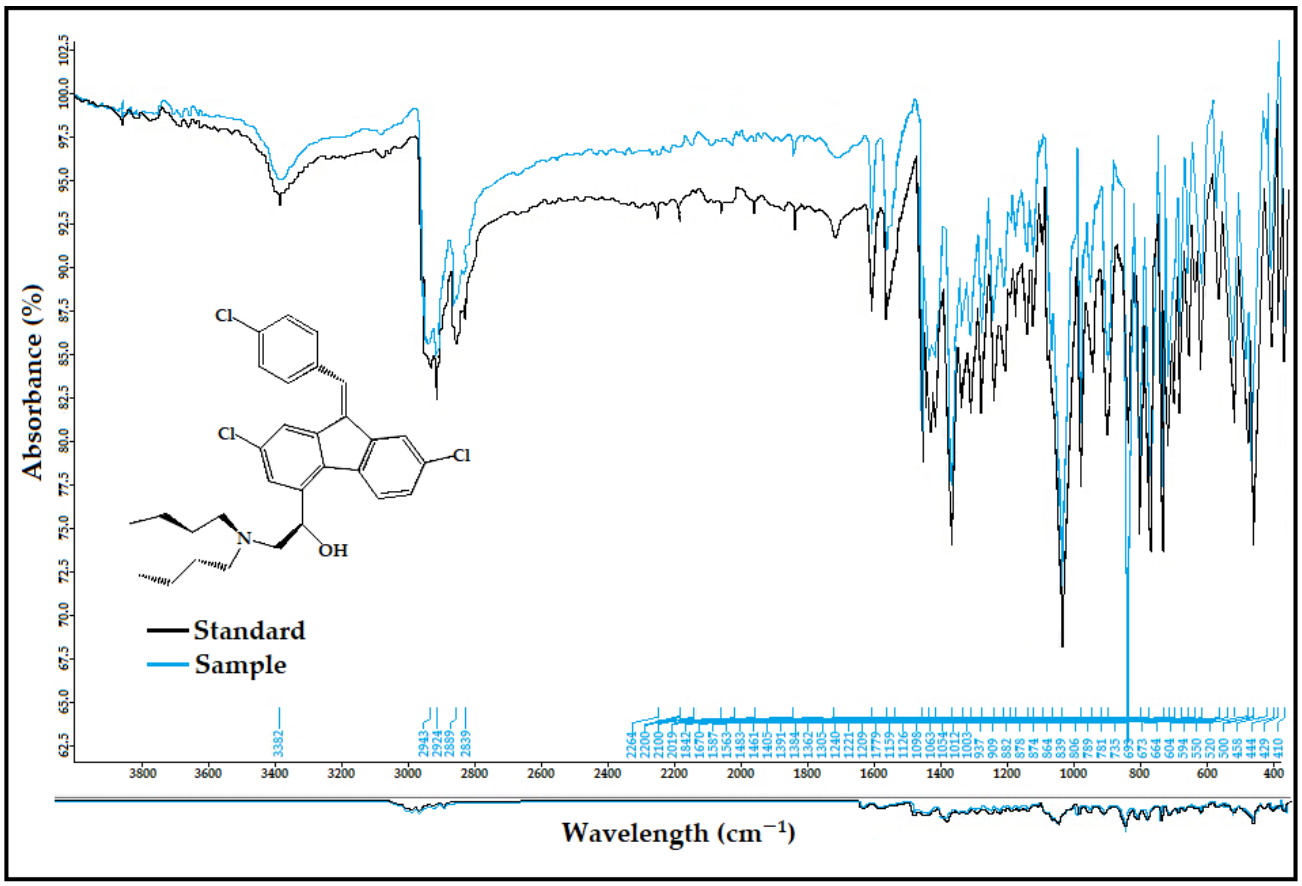

Fig. S2. Comparison of the IR spectra of the lumefantrine (LUM) used for research purposes and the LUM reference standard.

S2. Isothermal Microcalorimetry (IMC)

Compatibility studies between ART and LUM, as well as the different excipients used in the SEDDS formulations were performed by means of isothermal microcalorimetry (IMC). Calorimetry refers to measuring techniques that are used for direct determination of the rate of heat production, heat, and heat capacity as a function of temperature and time [1]. Microcalorimetry is a robust method for determining incompatibilities and instabilities between active pharmaceutical ingredients and/or excipients. This method is a credible way of detecting incompatibilities, because almost all physical and chemical processes are accompanied by heat exchange. Hence, it is sensitive to all physical and chemical processes associated with heat flow. The high sensitivity of this method renders it possible to conduct measurements at temperatures close to real conditions and to detect noticeably slow reactions. Heat flow data will contain inputs from either one process, or several processes. To differentiate specific contributions, careful experimental planning is mandatory, as well as sufficient background knowledge pertaining to the sample being analyzed [1].

First a baseline must be established prior to calculating the heat flow of the various components to determine if any interactions were detected. The baseline is calculated by individually measuring the heat flow of each component. Subsequently, ART, LUM and the selected oils and surfactants used were weighed and mixed in a 1:1:1:1:1 ratio. The various combinations were placed in the Thermal Activity Monitor (TAMIII) apparatus (TA Instruments, New Castle, Delaware, USA) for 24 h at 50°C. Next, each of the combinations were compared to the baseline values. The calorimetric output of the individual components is summarized as the hypothetical response. This hypothetical response is the anticipated calorimetric output if the two components measured do not interact with each other. If an interaction is observed, the observed calorimetric output will differ notably from the hypothetical response.

Furthermore, an interaction between two or more components will be detected if the change in heat flow from the observed heat flow compared to the hypothetical response is higher than 100 µW/g or if any additional slopes or troughs on the graphs are visible.

Fig. S3 depicts the observed heat flow versus the hypothetical response for avocado oil (AVO) in combination with ART, LUM, and the selected surfactants. The interaction heat flows for the various graphs are: 4.78 ± 4.15 µW/g; 9.58 ± 3.85 µW/g; 14.12 ± 1.42 µW/g; and 19.91 ± 19.52 µW/g, respectively. These interaction heat flow values are, according to compatibility studies, noted as slightly higher values. However, because all the interaction heat flow values remain below 100 µW/g; and due to the fact that no troughs are seen on the interaction curves, no incompatibilities could be identified, and the combinations are consequently deemed compatible.

In a similar fashion, castor oil's (CAS) heat flow measurements were compared to ART, LUM, and the selected surfactants to ascertain whether any interactions coexist between these various components. Fig. S4 exhibits the observed normalized heat flows versus the hypothetical responses for the different CAS combinations. The interaction heat flow values attained for the different combinations are: 4.92 ± 9.93 µW/g, 9.70 ± 11.4 µW/g, 20.58 ± 27.06 µW/g, and 1.29 ± 4.02 µW/g, individually. All the acquired interaction heat flow results are again below 100 µW/g with no additional slopes or troughs on the graphs. It can therefore be concluded that no interaction was observed between CAS and the various components.

Results obtained in terms of interaction heat flow data of coconut oil (CCT) combinations are portrayed in Fig. S5. The interaction heat flow values for these combinations are: 12.67 ± 12.78 µW/g, 11.99 ± 12.40 µW/g, 15.32 ± 16.60 µW/g, and 5.44 ± 6.42 µW/g, correspondingly. The calculated interaction heat flow values of the said combinations are again a little high comparatively, but still below 100 µW/g, hence, proving that the different components are compatible with one another. There is a small endothermic event visible in both Fig. S5 (c) and (d); nonetheless, these events are not an indication that an incompatibility was detected as these changes in heat flow may be considered relatively small (15.32 ± 16.60 µW/g and 5.44 ± 6.42 µW/g) and thus seen as negligible.

Following, the interaction heat flow results for combinations of olive oil (OLV), ART, LUM, and the selected surfactants are shown in Fig. S6. Interaction heat flow values achieved for these combinations are 5.37 ± 6.55 µW/g; 1.15 ± 1.49 µW/g; 24.75 ± 21.52 µW/g; and 7.12 ± 6.58 µW/g, respectively, with no slopes or troughs visible, which indicated that no incompatibilities were detected.

Last, the various combinations of peanut oil (PNT) with the active ingredients and selected surfactants are displayed in Fig. S7. No incompatibilities were again detected as no slopes or troughs were present and the interaction heat flow values calculated for each combination are: 698.1 nW/g ± 9.24 nW/g, 16.91 ± 17.31 µW/g, 21.57 ± 24.54 µW/g, and 8.77 ± 9.34 µW/g, separately. These values are once again below 100 µW/g, thus confirming that these components are compatible.

Overall, no incompatibilities were detected between any oil, drug, or surfactant combination, rendering all the combinations ideal for the purpose of formulating SEDDSs containing a fixed-dose of ART and LUM. When formulating emulsions, it is vital that the components are all compatible so as not to influence the stability of a given formulation, which could further compromise the integrity of these formulations. For example, if incompatibilities exist, the zeta potential of the emulsion will most probably also be affected, causing oil droplets to aggregate which can cause flocculation or coalescence [2]. Furthermore, a change in the physicochemical properties of the components can affect the pH of an emulsion, which in turn may lead to a change in color as well as the emulsion becoming rancid [3]. All these aforementioned factors can cause instability within an emulsion, initiating flocculation, creaming, phase separation, Ostwald ripening, and/or coalescence. Hence, emphasizing the importance that all the drugs and excipients should be compatible to maintain the integrity of a given emulsion [2,4].

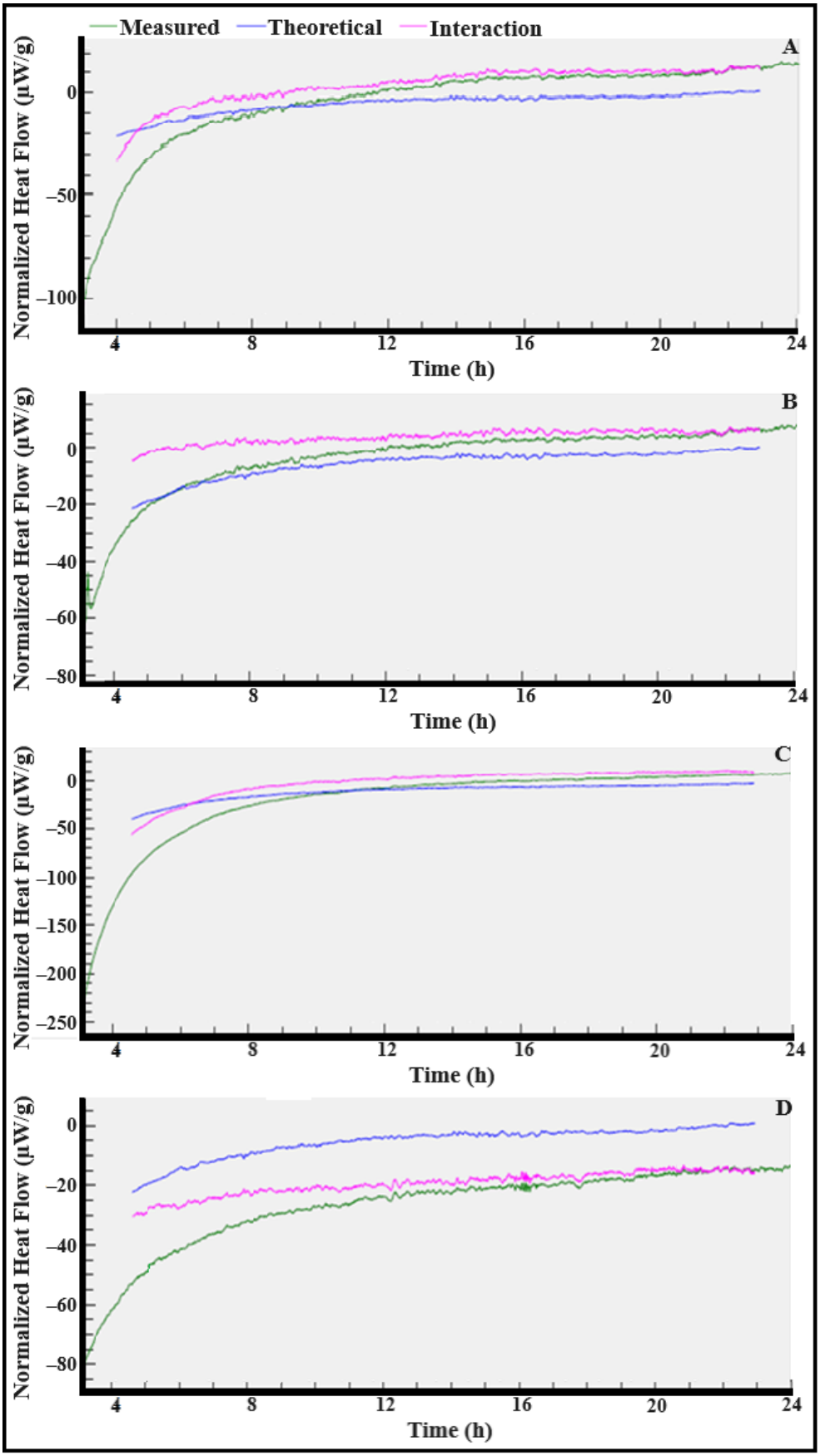

Fig. S3. Heat flow data attained from the combinations. (A) Artemether (ART), Lumefantrine (LUM), Avocado Oil, Tween®80 and Span®60; (B) ART, LUM, Avocado Oil, Tween®80 and Span®80; (C) ART, LUM, Avocado Oil, Sodium Lauryl Sulphate (SLS) and Span®60; and (D) ART, LUM, Avocado Oil, SLS and Span®80. All combinations were assessed in a 1:1:1:1:1 ratio.

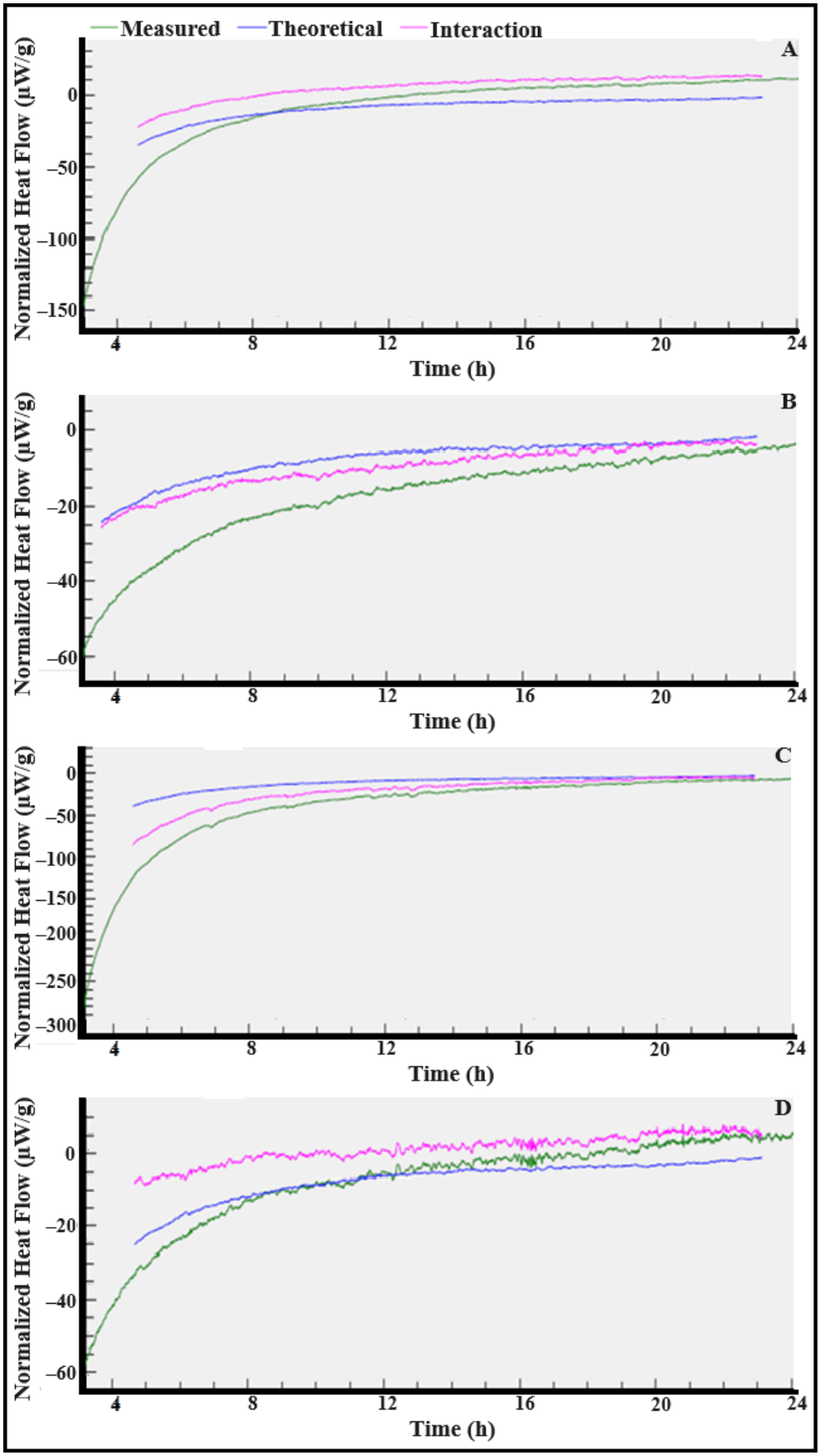

Fig. S4. Heat flow data acquired with the combinations. (A) Artemether (ART), Lumefantrine (LUM), Castor Oil, Tween®80 and Span®60; (B) ART, LUM, Castor Oil, Tween®80 and Span®80; (C) ART, LUM, Castor Oil, Sodium Lauryl Sulphate (SLS) and Span®60; and (D) ART, LUM, Castor Oil, SLS and Span®80. All combinations were tested in a 1:1:1:1:1 ratio.

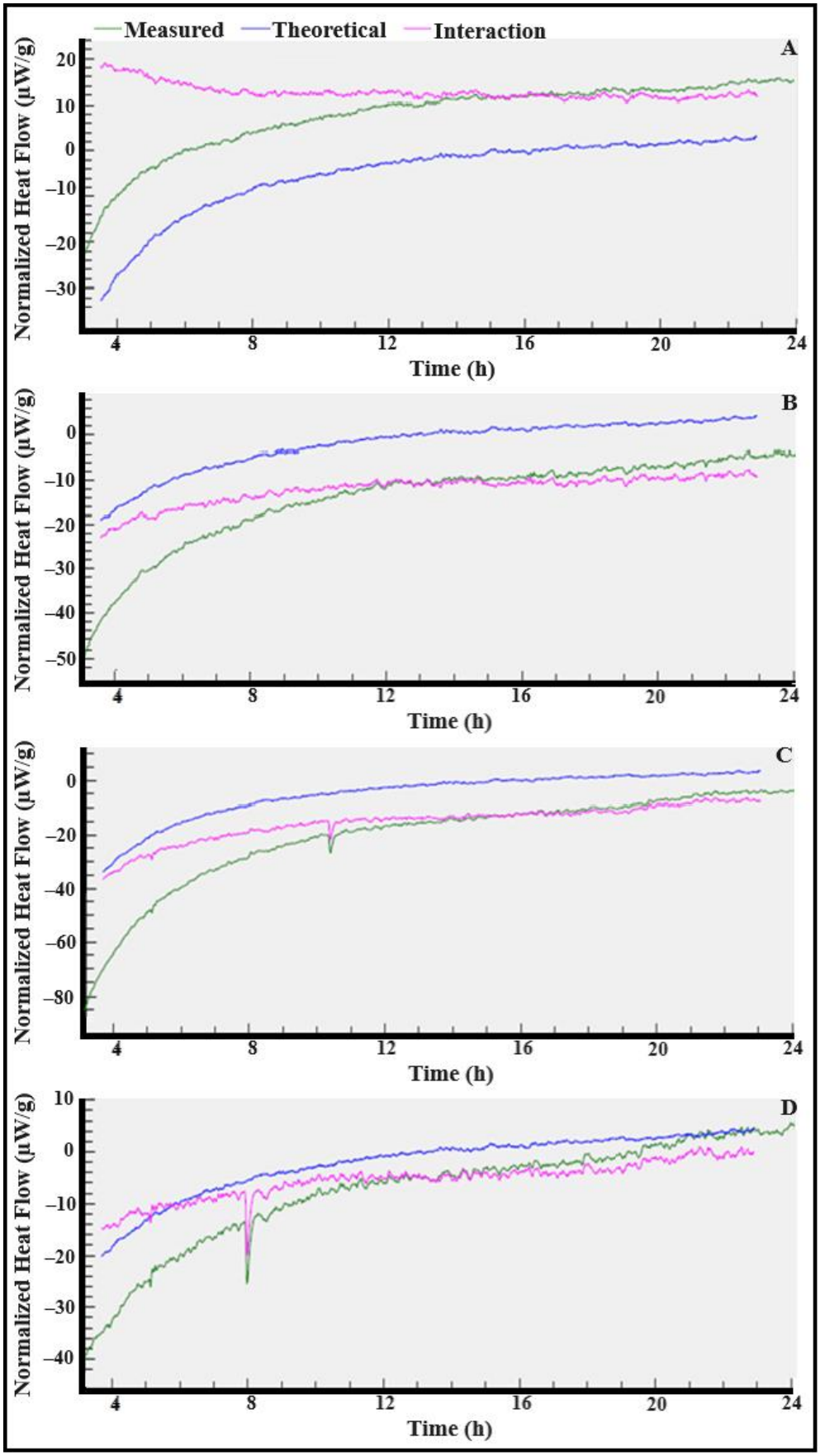

Fig. S5. Heat flow data achieved from the following blends: (A) Artemether (ART), Lumefantrine (LUM), Coconut Oil, Tween®80 and Span®60; (B) ART, LUM, Coconut Oil, Tween®80 and Span®80; (C) ART, LUM, Coconut Oil, Sodium Lauryl Sulphate (SLS) and Span®60; and (D) ART, LUM, Coconut Oil, SLS and Span®80. All combinations were assessed in a 1:1:1:1:1 ratio.

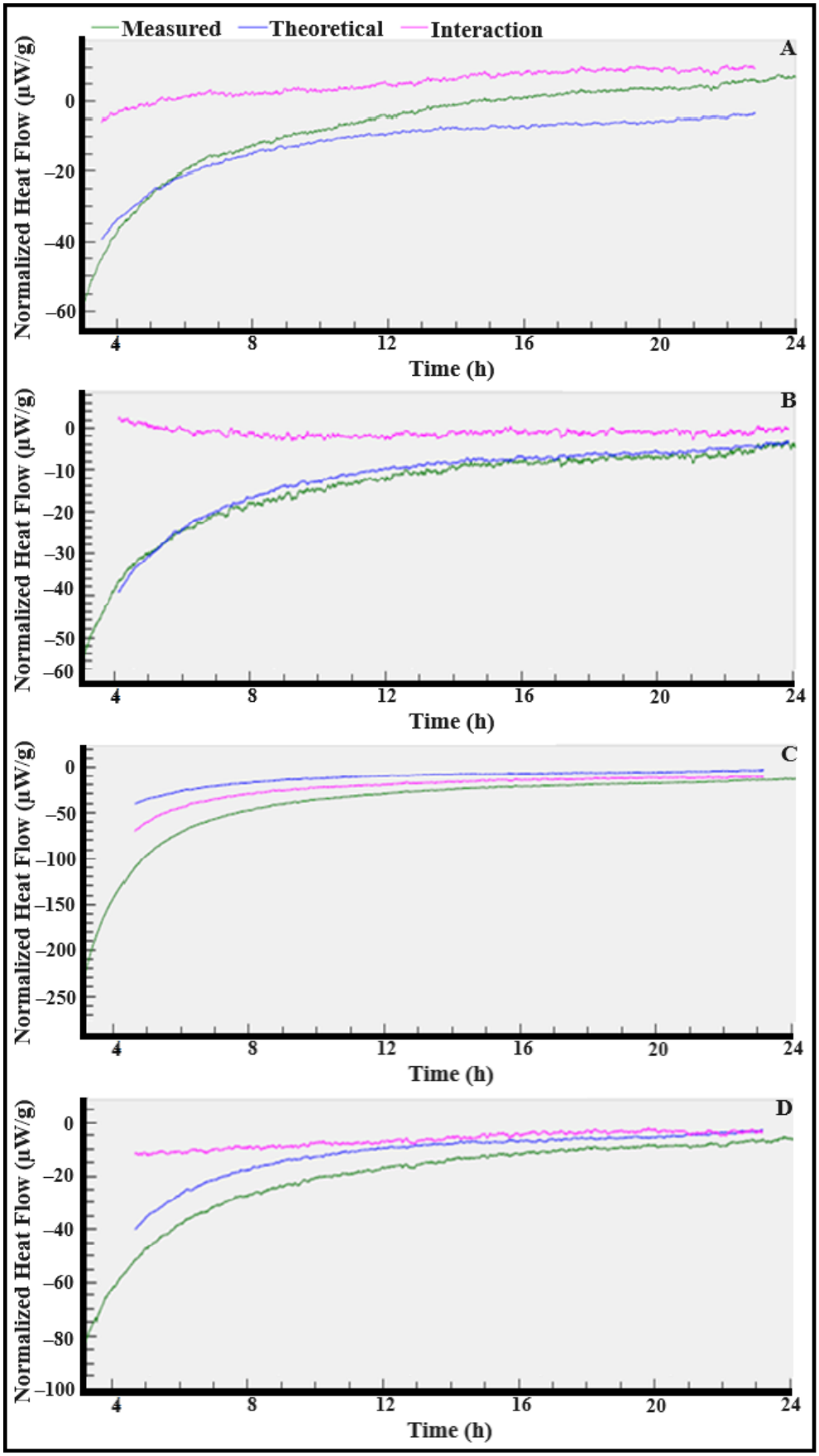

Fig. S6. Heat flow data obtained with the combinations. (A) Artemether (ART), Lumefantrine (LUM), Olive Oil, Tween®80 and Span®60; (B) ART, LUM, Olive Oil, Tween®80 and Span®80; (C) ART, LUM, Olive Oil, Sodium Lauryl Sulphate (SLS) and Span®60; and (D) ART, LUM, Olive Oil, SLS and Span®80. All combinations were tested in a 1:1:1:1:1 ratio.

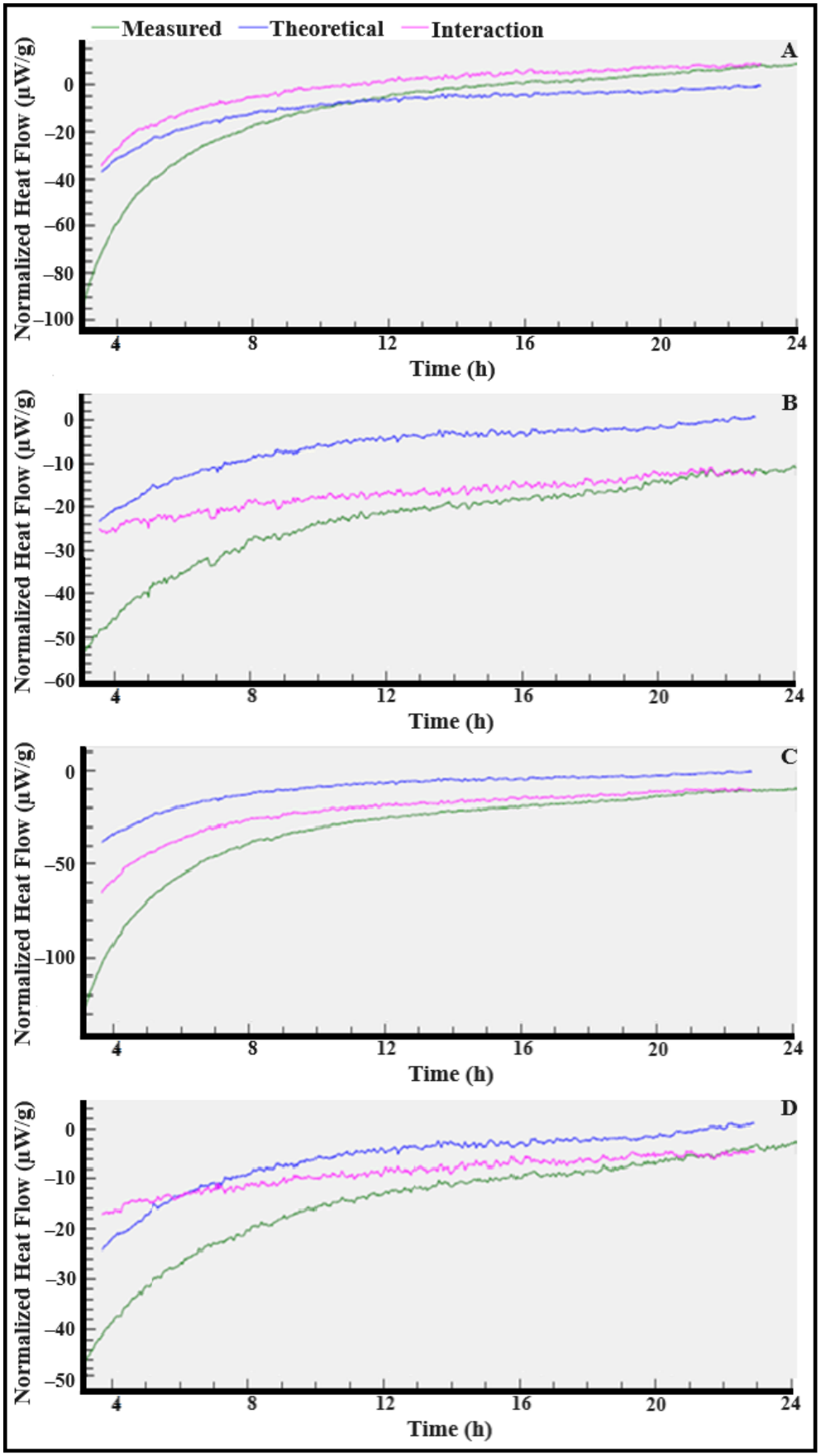

Fig. S7. Heat flow data obtained from the following blends: (A) Artemether (ART), Lumefantrine (LUM), Peanut Oil, Tween®80 and Span®60; (B) ART, LUM, Peanut Oil, Tween®80 and Span®80; (C) ART, LUM, Peanut Oil, Sodium Lauryl Sulphate (SLS) and Span®60; and (D) ART, LUM, Peanut Oil, SLS and Span®80. All combinations were assessed in a 1:1:1:1:1 ratio.

S3. Pseudo-ternary Phase Diagrams

SEDDSs will form oil-in-water emulsions with only moderate agitation once these systems are introduced into an aqueous media. The selected surfactant and co-surfactant(s) adsorb at the interface with subsequent reduction of the interfacial energy. Consequently, the thermodynamic stability of the formulation is improved by means of a decrease in the free energy required to form the emulsion. The selection of the oil and surfactant phases therefore plays a vital role in the design of SEDDS formulations [5]. Pseudo-ternary phase diagrams of the oils, surfactant, co-surfactants, and water may be extremely supportive in determining the most appropriate composition of SEDDSs. These diagrams identify the self-emulsifying regions and furthermore determine the optimum concentrations and ratios of oil, surfactant and co-surfactant when used in a combination. Once the region of a SEDDS is established, the feasibility of forming an emulsion can be determined [5,6].

In order to find an appropriate concentration range for all the components at room temperature (approximately 25°C) in which they spontaneously form emulsions, pseudo-ternary phase diagrams were constructed utilizing the water titration method [5–7]. First, the surfactant and co-surfactant were mixed. This mixture is referred to as the "surfactant phase". Kang et al. [8] determined that the ratio of surfactant and co-surfactant should be 1:1 as they found that higher concentration ratios improved the emulsion range, however, a decrease in stability was noted which could lead to precipitation of the incorporated drug. Next, mixtures of the oil and surfactant phases at certain weight ratios (w/w) of 10:0, 9:1, 8:2, 7:3, 6:4, 5:5, 4:6, 3:7, 2:8, 1:9 and 0:10, in different glass vials, were moderately agitated by means of vortexing for 5 min to form homogenous mixtures. Each mixture was titrated with water in a dropwise fashion until the first sign of turbidity was noted so as to identify the endpoint of the emulsion range. Post equilibrium, if the system became clear, the addition of water was continued. Once equilibrium of the mixture was achieved, the combinations were visually inspected by means of polarized lenses for transparency and for optical isotropicity. Inspection of the SEDDSs through a polarized lens is a simple way to generally classify a SEDDS. If the observed solution is black, the SEDDS is categorized as being in the microemulsion range. However, particle size analysis, utilizing a Zetasizer Nano ZS (Malvern Instruments, Worcestershire, UK), was also performed to undoubtedly classify the different SEDDSs [5–7,9,10].

Next, the pseudo-ternary phase diagrams were constructed. In these diagrams a range is highlighted where a selected oil and surfactant in conjunction with water formulate a stable SEDDS. The diagram consists of three well-defined regions: the uncolored region representing the coarse dispersion region; the light green area indicating the liquid crystal region; and the dark green region signifying the nano-emulsion area. Based on visual inspection, mixtures that were composed of a selected oil and either the Tween®80/Span®60 or the Tween®80/Span®80 surfactant phase, and which formed SEDDSs that seemed to adhere to the set criteria after the water phase was added, were analyzed further. Furthermore, the different oil phases of the SEDDS formulations that completely solubilized the fixed-dose ART and LUM, were selected for further stability investigation. These SEDDS formulations were again prepared and left to stand for 24 h to establish whether phase separation would occur within these formulations. All the SEDDS formulations that contained the Tween®80/Span®80 surfactant phase as well as the castor oil SEDDS, which consisted of the Tween®80/Span®60 surfactant phase, formed stable emulsions. These formulations could therefore be further analyzed. On the other hand, SEDDSs that comprised the surfactant Tween® 80 and co-surfactant Span® 60 displayed phase separation (Fig. S8).

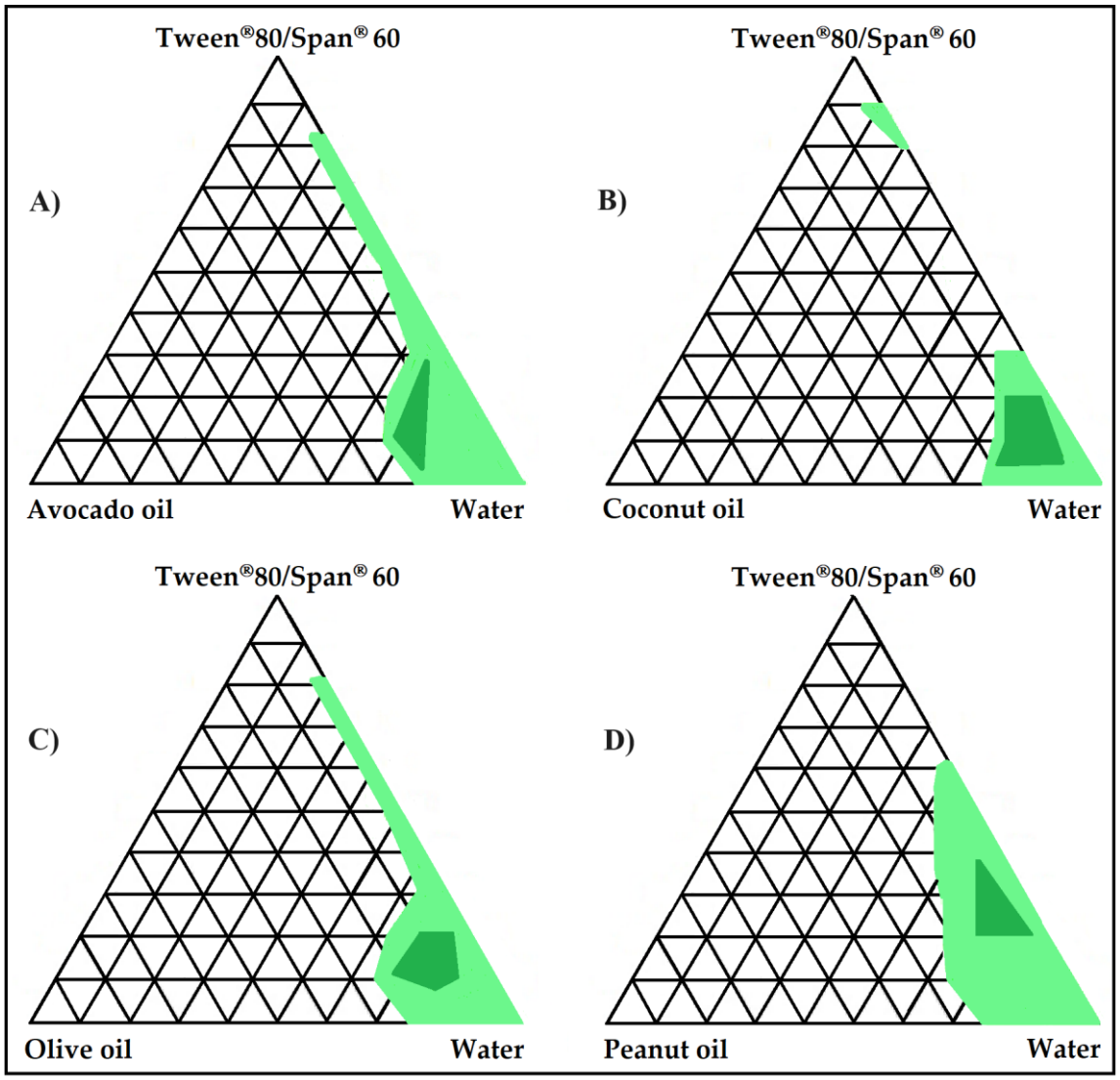

Fig. S8. Pseudoternary phase diagrams showing mixtures of the unstable SEDDSs that formed. (A) Avocado Oil, Tween®80/Span®60, and water; (B) Coconut Oil, Tween®80/Span®60, and water; (C) Olive oil, Tween®80/Span®60, and water; and (D) Peanut oil, Tween®80/Span®60, and water. The uncolored region represents the coarse dispersion region. The green area signifies the single-phase emulsion region, where the light green area indicates the liquid crystal region; and the dark green region denotes the nanoemulsion area.

It was also clear that SEDDSs which constituted sodium lauryl sulphate and Span®80 as the surfactant phase (Fig. S9) could not be deemed acceptable for further study as these systems produced SEDDSs with too narrow ranges to experiment with; or the SEDDS formulations that developed upon preparation, were not stable or clear. The reason for sodium lauryl sulphate not forming a proper emulsion range can most likely be attributed to the hydrophile-lipophile balance (HLB) value of this surfactant. As stated, the choice of surfactants plays an imperative role in the emulsification of SEDDSs, moreover, the HLB value of the oil has also been acknowledged as a vital component in the emulsification process [11–13]. Theoretically, the HLB system acts as a scientific approach in predicting the best surfactant and co-surfactant required to produce an optimal emulsifying system. An optimal emulsifying system is formed when the HLB values of the oil and surfactant phases match [10–14]. Consequently, if the HLB values of the surfactant phase coincide with the HLB values of the oil phase, a stable emulsion will form. Sodium lauryl sulphate has an HLB value of 40 (significantly hydrophilic), which is notably higher than the values of Span®80 (HLB = 4.3)

as well as each of the oils, having HLB values ranging from 6–12 [14]. Consequently, these values did not match, rendering sodium lauryl sulphate too hydrophilic to stabilize the different oil phases when combined with the water phase.

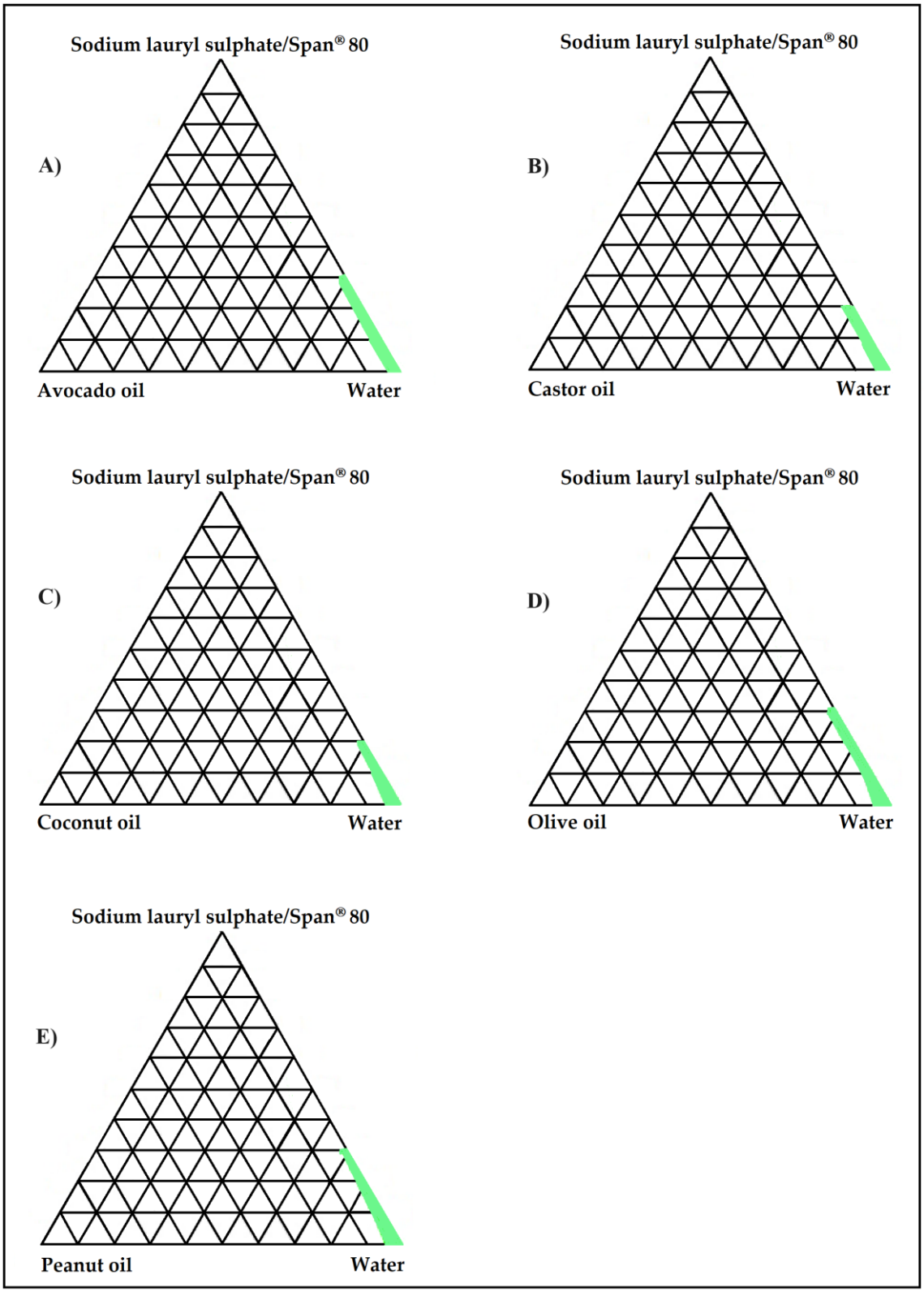

Fig. S9. Pseudoternary phase diagrams demonstrating the unstable SEDDSs. (A) Avocado oil, Sodium Lauryl Sulphate (SLS)/Span®80, and water system; (B) Castor Oil, SLS/Span®80, and water system; (C) Coconut Oil, SLS/Span®80, and water system; (D) Olive Oil, SLS/Span®80, and water system; and (E) Peanut Oil, SLS/Span®80, and water system. The green dispersion areas of the different systems are so small that the single-phase emulsion region could not be properly differentiated.

S4. Fit Factors: Indicating Similarities and Differences Between Tested Formulations

Fit factors were used to compare the dissolution profiles of the sample formulations to a control formulation (Coartem®). Fit factor, f_1, is defined as the difference factor and establishes the percentage error between two curves. Curves that are identical will have a f_1 value of 0. As this value increases, so does the variation between the two curves. For dissolution curves to be considered comparable, the f_1 value should be ≤ 15, indicating that the amount of time taken to dissolve the drug correlates for both the sample and control formulations. Fit factor, f_2, conversely, is an indication of the similarity between two curves. If this value is ≥ 50 it suggests that both the sample and control formulations are fairly similar. If the value obtained for f_2 is equal to 100, the two curves are deemed identical [15].

Considering all the fit factors obtained (Table S1) to ascertain whether significant differences concerning the release profiles of ART from the selected SEDDS formulations could be detected, it was found that all the ART release profiles differed statistically significantly from the ART release profile from Coartem®. ART was released notably faster from Coartem® (MDT value = 235.252 min) compared to the SEDDSs. Furthermore, it could be concluded that only the SEDDSs that comprised castor oil (CAS2:8S80 and CAS3:7S60), regardless the surfactant phase included, differed statistically significantly (f_1 >15; f_2 <50) from the other SEDDS formulations. The castor oil SEDDSs overall displayed longer delayed ART release profiles as well as higher and faster ART release once drug release was initiated.

Table S1. Fit factors assessed for ART release, demonstrating statistically significant differences in red and similarities in blue.

Formulation		Coartem®	AVO4:6[1]	CAS2:8S80[2]	CAS3:7S60[3]	CCT6:4[4]	OLV3:7[5]	PNT6:4[6]
Coartem®	f_1		64.276	32.762	26.372	43.127	46.797	39.381
	f_2		34.894	32.602	38.681	32.752	30.363	34.872
AVO4:6[1]	f_1	64.276		38.579	36.041	12.197	14.840	9.104
	f_2	34.894		42.101	44.454	64.662	63.111	72.216
CAS2:8S80[2]	f_1	32.762	38.579		15.067	30.583	45.315	35.166
	f_2	32.602	42.101		52.472	43.773	41.869	44,503
CAS3:7S60[3]	f_1	26.372	36.041	15.067		39.220	49.511	33.574
	f_2	38.681	44.454	52.472		44.282	41.255	46,702
CCT6:4[4]	f_1	43.127	12.197	30.583	39.220		16.883	7.576
	f_2	32.752	64.662	43.773	44.282		62.575	76.321
OLV3:7[5]	f_1	46.797	14.840	45.315	49.511	16.883		18.791
	f_2	30.363	63.111	41.869	41.255	62.575		61.081
PNT6:4[6]	f_1	39.381	9.104	35.166	33.574	7.576	18.791	
	f_2	34.872	72.216	44,503	46,702	76.321	61.081	

[1]AVO4:6 = Avocado Oil + Tween®80/Span®80 in a 4:6 ratio; [2]CAS2:8S80 = Castor Oil + Tween®80/Span®80 in a 2:8 ratio; [3]CAS3:7S60 = Castor Oil + Tween®80/Span®60 in a 3:7 ratio; [4]CCT6:4 = Coconut Oil + Tween®80/Span®80 in a 6:4 ratio; [5]OLV3:7 = Olive Oil + Tween®80/Span®80 in a 3:7 ratio; [6]PNT6:4 = Peanut Oil + Tween®80/Span® in a 6:4 ratio.

Pertaining to dissolution profiles evaluated for LUM release and dissolution, it was recognized that the LUM concentration dissolved could not be quantified for the commercial product, Coartem®. Thus, no comparison in terms of the fit factors between the SEDDS formulations with the control could be made. LUM was furthermore released significantly slower and to a lesser extent when compared to ART release ($p \leq 0.05$) during the same period. No statistically significant differences ($f_1 < 15$; $f_2 > 50$) regarding LUM release could be determined between AVO4:6; CCT6:4; OLV3:7; or PNT6:4 (Table S2). Additionally, the fit factors once again, indicated that only the castor oil containing SEDDSs (CAS2:8S80 and CAS3:7S60) depicted statistically significant differences from the other SEDDS formulations in respect of their release profiles. These formulations did however portray similar delayed LUM release profiles ($f_1 = 3.995$; $f_2 = 96.554$), but the LUM concentrations released from these two formulations were significantly lower ($f_1 > 15$; $f_2 < 50$) compared to the other SEDDSs (Table S2).

Table S2. . Fit factors assessed for LUM release, indicating statistically significant differences in red and similarities in blue.

Formulation		AVO4:6[1]	CAS2:8S80[2]	CAS3:7S60[3]	CCT6:4[4]	OLV3:7[5]	PNT6:4[6]
AVO4:6[1]	f_1		45.553	44.299	23.703	7.253	9.264
	f_2		53.277	53.535	63.949	85.537	82.649
CAS2:8S80[2]	f_1	45.553		3.995	40.131	41.424	39.043
	f_2	53.277		96.554	69.844	55.720	58.709
CAS3:7S60[3]	f_1	44.299	3.995		26.995	40.075	40.416
	f_2	53.535	96.554		71.210	56.114	58.196
CCT6:4[4]	f_1	23.703	40.131	26.995		17.917	16.504
	f_2	63.949	69.844	71.210		66.854	73.354
OLV3:7[5]	f_1	7.253	41.424	40.075	17.917		7.420
	f_2	85.537	55.720	56.114	66.854		86.100
PNT6:4[6]	f_1	9.264	39.043	40.416	16.504	7.420	
	f_2	82.649	58.709	58.196	73.354	86.100	

[1]AVO4:6 = Avocado Oil + Tween®80/Span®80 in a 4:6 ratio; [2]CAS2:8S80 = Castor Oil + Tween®80/Span®80 in a 2:8 ratio; [3]CAS3:7S60 = Castor Oil + Tween®80/Span®60 in a 3:7 ratio; [4]CCT6:4 = Coconut Oil + Tween®80/Span®80 in a 6:4 ratio; [5]OLV3:7 = Olive Oil + Tween®80/Span®80 in a 3:7 ratio; [6]PNT6:4 = Peanut Oil + Tween®80/Span® in a 6:4 ratio.

S5. Pharmacokinetics of the Release Profiles Pertaining to the Formulated Self-emulsifying Drug Delivery Systems

In vitro dissolution analysis is not only utilized to direct the reliability and stability of drug delivery systems, but it can additionally be used as a reasonably fast and inexpensive technique to calculate *in vivo* absorption of a said drug. For these reasons, quantitative assessment of drug dissolution properties is of immense interest; and although a wide variety of mathematical models exist to fit drug release results, all of these are achieved by means of nonlinear equations. “DDSolver” is a menu-driven add-in program for Microsoft Excel written in “Visual Basic for Applications” and may be retained to ease drug release model fitting. The purpose of fitting a dissolution profile to

mathematic modelling is to simplify the complex release profile of a drug and gain comprehension into the release mechanism of a specific dosage form [16].

The release kinetics of both ART and LUM were fitted with DDSolver to all the models applied in the program. Lag time release properties were also considered. The DDSolver program offers various statistical principles for analyzing the goodness of fit of a model. These include the correlation coefficient, the coefficient of determination, the adjusted coefficient of determination, the mean square error, the standard deviation of the residuals, sum of squares, weighted sum of squares, the Akaike Information Criterion, and the Model Selection Criterion (MSC). However, for the release kinetics of ART and LUM assessed in this study; and to identify the best fitted model, the correlation coefficient (r^2) and the MSC were employed. The best fit of the drug release profile is the model where the calculated r^2 approaches a value of 1, in other words, the highest r^2 value; and also, where the largest MSC value is obtained. In general, a MSC value of more than two to three designates a good fit [16,17].

Table S3. Release kinetics of Artemether (ART) and Lumefantrine (LUM) from the selected SEDDS formulations in sequential dissolution media, including biorelevant components, fitted to different mathematical models. The r^2 values are defined as the correlation coefficients, MSC values are considered the model selection criterion, and k_1 is the Fickian diffusion constant.

	SEDDS	r^2	MSC	k_1
ART	AVO4:6[1]	0.997	5.028	1.030
	CAS2:8S80[2]	0.996	4.710	6.578
	CAS3:7S60[3]	0.997	5.037	5.414
	CCT6:4[4]	0.997	4.867	3.338
	OLV3:7[5]	0.994	3.374	2.378
	PNT6:4[6]	0.995	4.576	2.794
LUM	AVO4:6[1]	0.991	4.021	2.035
	CAS2:8S80[2]	0.999	6.991	2.386
	CAS3:7S60[3]	0.999	8.005	2.003
	CCT6:4[4]	0.999	6.359	2.874
	OLV3:7[5]	0.995	3.586	1.708
	PNT6:4[6]	0.996	4.882	2.506

[1]AVO4:6 = Avocado Oil + Tween®80/Span®80 in a 4:6 ratio; [2]CAS2:8S80 = Castor Oil + Tween®80/Span®80 in a 2:8 ratio; [3]CAS3:7S60 = Castor Oil + Tween®80/Span®60 in a 3:7 ratio; [4]CCT6:4 = Coconut Oil + Tween®80/Span®80 in a 6:4 ratio; [5]OLV3:7 = Olive Oil + Tween®80/Span®80 in a 3:7 ratio; [6]PNT6:4 = Peanut Oil + Tween®80/Span® in a 6:4 ratio.

In Table S3 the r^2 and MSC values of all the selected SEDDS formulations are tabled. All the values are higher than 0.990 and 3, respectively; therefore, implying that the Peppas-Sahlin 2 model is the best fit for both ART and LUM release from the different SEDDS formulations tested. The Peppas-Sahlin model explains the release profile of a drug, fitting the release profile of the drug to either Fickian diffusional release or Case- II relaxational release. Fickian diffusion can be described as the solute transport process where the polymer relaxation time is greater than the solvent diffusion time. Fickian release ensues by molecular diffusion of the drug from the dosage form to the

gastrointestinal media due to a chemical potential gradient. If the Fickian diffusion constant (k_1) value is higher than 1, it can safely be assumed that Fickian diffusion transpired. Case- II relaxational release, conversely, is due to stresses and state-transition in hydrophilic glassy polymers that swell upon contact with biological fluids or water, in a similar fashion when a lipid swells upon contact with biological fluids [18]. Due to all the k_1 values being higher than 1, it is suggested that Fickian diffusion occurred from all the SEDDS formulations analyzed.

References

[1] Wadsö L. Operational Issues in Isothermal Calorimetry. Cement and Concrete Research. 2010; 40: 1129–1137. https://doi.org/10.1016/j.cemconres.2010.03.017.

[2] Fustier P, Taherian AR, Ramaswamy HS. Emulsion Delivery Systems for Functional Foods. In Smith J, Charter E (eds.) Functional Food Product Development (pp. 79–97). John Wiley & Sons Ltd, Publication: Charlottetown. 2010.

[3] Rousseau D. Fat Crystals and Emulsion Stability – A Review. Food Research International. 2000; 33: 3–14. https://doi.org/10.1016/S0963-9969(00)00017-x.

[4] Fatima M, Sheraz MA, Ahmed S, Kazi SH, Ahmad I. Emulsion Separation, Classification and Stability Assessment. Journal of Pharmaceutical Sciences. 2014; 2: 56–62. https://jpps.juw.edu.pk/index.php/jpps/article/view/53.

[5] Czajkowska-Kośnik A, Szekalska M, Amelian A, Szymańska E, Winnicka K. Development and Evaluation of Liquid and Solid Self-Emulsifying Drug Delivery Systems for Atorvastatin. Molecules. 2015; 20: 21010–21022. https://doi.org/10.3390/molecules201219745.

[6] Wang W, Wei H, Tai X, Wang G. Formation and Characterization of Fully Dilutable Microemulsion with Fatty Acid Methyl Esters as Oil Phase. ACS Sustainable Chemistry & Engineering. 2015; 3: 443–450. https://doi.org/10.1021/sc500667n.

[7] Boonme P, Krauel K, Graf A, Rades T, Junyaprasert VB. Characterization of Microemulsion Structures in the Pseudoternary Phase Diagram of Isopropyl Palmitate/Water/Brij 97:1-Butanol. AAPS PharmSciTech. 2006; 7: E45. https://doi.org/10.1208/pt070245.

[8] Kang BK, Lee JS, Chon SK, Jeong SY, Yuk SH, Khang G, *et al*. Development of Self-Microemulsifying Drug Delivery Systems (SMEDDS) for Oral Bioavailability Enhancement of Simvastatin in Beagle Dogs. International Journal of Pharmaceutics. 2004; 274: 65–73. https://doi.org/10.1016/j.ijpharm.2003.12.028.

[9] Joshi M, Pathak S, Sharma S, Patravale V. Solid Microemulsion Preconcentrate (NanOsorb) of Artemether for Effective Treatment of Malaria. International Journal of Pharmaceutics. 2008; 362: 172–178. https://doi.org/10.1016/j.ijpharm.2008.06.012.

[10] Wang Z, Pal R. Enlargement of Nanoemulsion Region in Pseudo-ternary Mixing Diagrams for a Drug Delivery System. Journal of Surfactants and Detergents. 2014; 17: 49–58. https://doi.org/10.1007/s11743-013-1497-6.

[11] Aboulfotouh K, Allam AA, El-Badry M, El-Sayed A. Development and *In Vitro*/*In Vivo* Performance of Self-nanoemulsifying Drug Delivery Systems Loaded with Candesartan Cilexetil. European Journal of Pharmaceutical Sciences. 2017; 109: 503–513. https://doi.org/10.1016/j.ejps.2017.09.001.

[12] Costa IC, Rodrigues RF, Almeida FB, Favacho HA, Falcão DQ, Ferreira AM, *et al*. Development of Jojoba Oil (Simmondsia Chinensis (link) C.K. Schneid.) Based Nanoemulsions. Latin American Journal of Pharmacy. 2014; 33: 459–63. chrome-extension://efaidnbmnnnibpcajpcglclefindmkaj/http://www.latamjpharm.org/resumenes/33/3/LAJOP_33_3_1_15.pdf.

[13] Wang L, Dong J, Chen J, Eastoe J, Li X. Design and Optimization of a New Self-Nanoemulsifying Drug Delivery System. Journal of Colloid and Interface Science. 2009; 330: 443–448. https://doi.org/10.1016/j.jcis.2008.10.077.

[14] Fernandes CP, Mascarenhas MP, Zibetti FM, Lima BG, Oliveira RPRF, Rocha L, *et al*. HLB Value, An Important

Parameter for the Development of Essential oil Phytopharmaceuticals. Revista Brasileira de Farmacognosia. 2012; 23: 108–114. https://doi.org/10.1590/S0102-695X2012005000127.

[15] Moore JW, Flanner HH. Mathematical Comparison of Dissolution Profiles. Pharmaceutical Technology. 1996; 20: 64–74. https://www.semanticscholar.org/paper/Mathematical-comparison-of-dissolution-profiles-Moore-Flanner/f637ff1a39fb1585970c4ef5ce43cd2170578c7d.

[16] Zhang Y, Huo M, Zhou J, Zou A, Li W, Yao C, *et al*. DDSolver: An Add-In Program for Modelling and Comparison of Drug Dissolution Profiles. The AAPS Journal. 2010; 12: 263–271. https://doi.org/10.1208/s12248-010-9185-1.

[17] Mayer BX, Mensik C, Krishnaswami S, Derendorf H, Eichler HG, Schmetterer L, *et al*. Pharmacokinetic-Pharmacodynamic Profile of Systemic Nitric Oxide-Synthase Inhibition with L-NMMA in Humans. British Journal of Clinical Pharmacology. 1999; 47: 539–44. https://doi.org/10.1046/j.1365-2125.1999.00930.x

[18] Fu Y, Kao WJ. Drug Release Kinetics and Transport Mechanisms of Non-Degradable and Degradable Polymeric Delivery Systems. Expert Opinion on Drug Delivery. 2010; 7: 429–444. https://doi.org/10.1517/17425241003602259.